DOI: 10.1002/ejoc.200800360

Synthesis and Phase Structures of Novel π-Acceptor Discotic Liquid Crystalline Compounds Having a Pyrenedione Core

Mikio Yasutake,[a] Takashi Fujihara,[a] Akira Nagasawa,[a] Keiichi Moriya,[b] and Takuji Hirose*[a]

Keywords: Liquid crystals / Lamellar phase / Arenes / Fused-ring systems / Semiconductors

Several π-acceptor discotic liquid crystalline compounds were synthesized by using a pyrenedione unit as a core. Terrace-like and band-like structures were revealed by polarized optical microscopy (POM) observations and XRD measurements. In conjunction with the results of the single-crystal structure analysis of analogous crystalline compounds, all of the liquid crystalline compounds were confirmed to form a discotic lamellar phase D_{L2}.

Introduction

Organic semiconductors have received much attention due to their high processability when compared with inorganic semiconductors.[1] Most organic semiconductors developed to date are planar and have a charge-transfer feature as a common characteristic. It is known that one-dimensional charge transport is possible by constructing a segregated columnar structure of donors and acceptors by the use of π–π interactions of aromatic structures.[2] In contrast, high conductivity is not expected for an alternative columnar structure of a charge-transfer (CT) complex. Recently, however, Saitou et al. found that a quinone–hydroquinone CT complex showed high electroconductivity due to a proton–electron transfer phenomenon, that is, simultaneous transfer of both electrons and protons, under high-pressure conditions.[3]

Liquid crystals are becoming increasingly important as organic semiconductors because it is easy to construct uniform and flexible devices with a large area.[4] Discotic liquid crystals are interesting candidates because electroconductivity is expected as a result of the movement of electrons and/or holes in the direction of the columns formed by piling up the discotic molecules.[5]

In a previous study, we synthesized several pyrene derivatives with acyloxy groups as discotic liquid crystalline compounds with a low melting temperature and high solubilities. Although crystalline themselves, they form columnar phases as CT complexes with a strong electron-acceptor core, tetranitrofluorenone, and they also change their textures depending on the side-chain structures.[6] On the basis of these results, we aimed to synthesize quinone–hydroquinone CT liquid crystalline systems that form segregated columnar structures and show high electroconductivity by using a pyrene moiety as the core. Here, we report on the first synthesis and the phase structures of π-acceptor liquid crystalline aromatic compounds having *anti*- and *syn*-pyrenedione moieties.

Results and Discussion

The synthesis of dioctyloxypyrenedione **4b** was attempted by typical ether synthesis from dihydroxypyrene derivative **3**. However the mixture of *anti* and *syn* derivatives, **4b** and **5b**, were obtained in low yields with tetraalkoxypyrene (Scheme 1).

Therefore, an alternative route was applied for the synthesis of **4** as shown in Scheme 2. Pyrene-1,6-dione **7** and pyrene-1,8-dione **8** were prepared in a 1:1 ratio (55% yield) by the oxidation of pyrene with sodium dichromate in 3 M H_2SO_4.[7] The mixture was treated with an alcohol in the presence of $FeCl_3$ to prepare corresponding alkoxy pyrene derivatives **4** and **5** in 23–38% yields.[8] Yellow *anti* derivatives **4a**–**d** were synthesized to study the relationship between the length of the side chain and the liquid crystallinity, and crystalline **4e** was synthesized as a model compound to clarify the crystal structure.

The HOMO and LUMO energy levels of **4c** and **5c** were estimated from cyclic voltammetry (CV) measurements and UV/Vis spectra. Compound **4** could have two reduction potentials, but, in this case, only the first one at –0.67 V (vs. Fc/Fc^+ in DMF) was determined from the quasireversible response shown in Figure 1a. The reduction potential corre-

[a] Graduate School of Science & Engineering, Saitama University, 255 Shimo-okubo, Sakura-ku, Saitama 338-8570, Japan
Fax: +81-48-858-9534
E-mail: hirose@apc.saitama-u.ac.jp
[b] Department of Chemistry, Faculty of Engineering, Gifu University,
1-1 Yanagido, Gifu 501-1193, Japan
Supporting information for this article is available on the WWW under http://www.eurjoc.org or from the author.

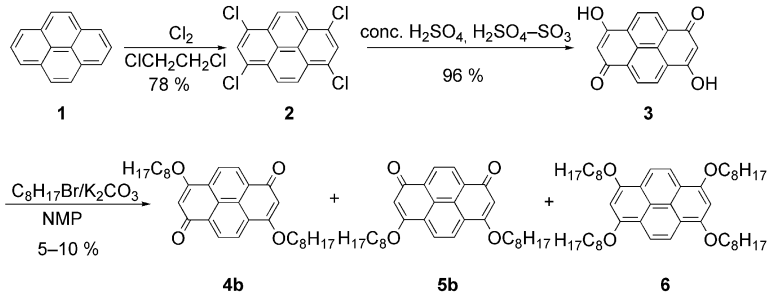

Scheme 1. Synthetic route to **4b** and **5b**.

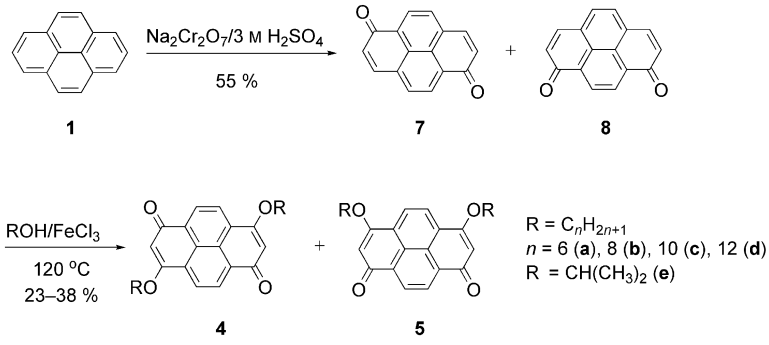

Scheme 2. Synthetic route to **4** and **5**.

sponds to a LUMO energy level of –4.13 eV.[9] The oxidation potential was not available from the CV measurement as a result of precipitation on the cathode. Therefore, the HOMO level was estimated to be approximately –6.98 eV from the absorption around 435 nm in the UV/Vis spectrum (Figure 2) and the LUMO energy level (E_{HOMO} = E_{LUMO} – transition energy).[10]

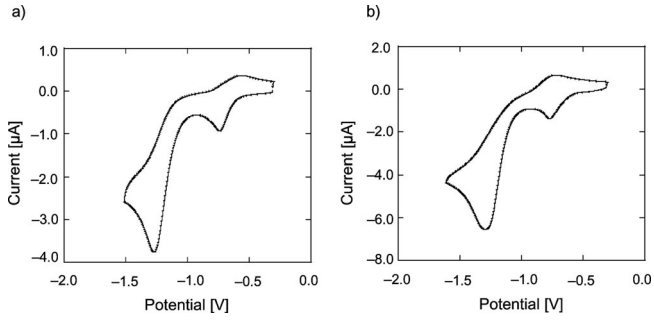

Figure 1. Cyclic voltammogram of (a) **4c** and (b) **5c** in DMF containing 0.1 M Bu_4NClO_4 at a scan rate of 20 mV s^{-1}. Electrodes: working, glassy carbon; counter, Pt; reference Ag/Ag$^+$ (0.1 M ClO_4^-).

Compound **5c** showed only the first reduction potential at –0.75 V (vs. Fc/Fc$^+$ in DMF) as well (Figure 1b), which corresponds to a LUMO energy level of –4.11 eV. The oxidation potential was not available either. Therefore, the HOMO level was estimated to be approximately –6.83 eV from the λ_{max} around 456 nm and the LUMO energy level.

The electronic states of **4c** and **5c** were calculated by ZINDO CI by using the structure coordinates optimized by MOPAC-AM1.[11] As expected, the electron density distribution of **4c** was symmetrical so that the molecular dipole moment was small (0.02 D). Contrastively, as seen in Figure 3, the dipole moment of **5c** was large (7.57 D).

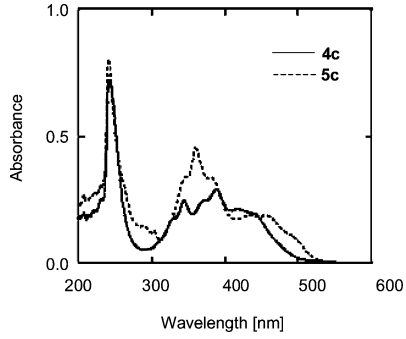

Figure 2. UV/Vis spectra of **4c** and **5c** in $CHCl_3$ (4.95×10^{-5} M).

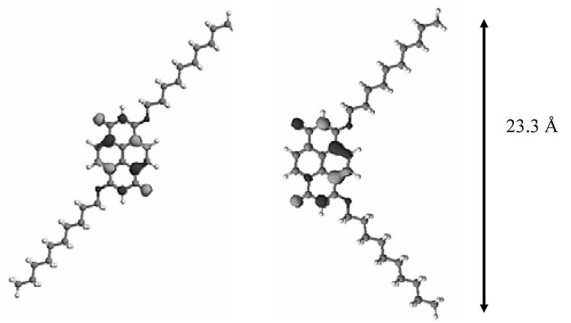

Figure 3. Electron density of the HOMOs of (a) **4c** and (b) **5c** by MOPAC-AM1 and ZNDO CI calculations.

The thermal properties of **4a**–**d** and **5a**–**d** were studied by DSC measurements, and it was found that several compounds showed monotropic phase transitions. The results of the cooling process are summarized in Table 1 for **4a**–**d** and in Table 2 for **5a**–**d**.

Table 1. Phase-transition temperatures and enthalpies of **4a**–**d**.[a]

Compound	Transition	Temperature [°C]	ΔH [kJ mol^{-1}]
4a	Iso → Cr	212	24
4b	Iso → Cr	207	27
4c	Iso → D_{L2}	208	8.6
	D_{L2} → Cr	184	17
4d	Iso → D_{L2}	184	26
	D_{L2} → Cr	74	40

[a] Cooling processes, cooling rate = 5 °C min^{-1}; Iso: isotropic, Cr: crystalline, D_{L2}: discotic lamellar.

Table 2. Phase-transition temperatures and enthalpies of **5a**–**d**.[a]

Compound	Transition	Temperature [°C]	ΔH [kJ mol^{-1}]
5a	Iso → Cr	178	22
5b	Iso → D_{L2}	170	14
	D_{L2} → Cr	134	28
5c	Iso → D_{L2}	148	16
	D_{L2} → Cr	106	27
5d	Iso → D_{L2}	139	11
	D_{L2} → Cr	105	34

[a] Cooling processes: cooling rate = 5 °C min^{-1}; Iso: isotropic, Cr: crystalline, D_{L2}: discotic lamellar.

Although **4c** and **4d** showed mesophases at 208–184 and 184–74 °C, respectively, **4a** and **4b** had only an isotropic-crystalline (Iso-Cr) transition. In contrast, **5b**–**d** showed mesophases at 170–134, 148–105, and 139–104 °C, respectively. Longer alkoxy chains were shown to be effective in causing a liquid crystalline phase to form and in controlling their phase transitions and temperatures.

Compounds **4a**–**d** and **5a**–**d** did not form single crystals. In order to consider the molecular arrangements of **4** and **5**, single-crystal X-ray analysis of **4e** and **5e** was carried out, and the results are shown in Figures 4–7.[12a]

The molecules of **4e** are stacked in parallel along the *a* axis to form a columnar structure (Figure 4a). The molecular distance in the column is about 3.52 Å, where π–π stacking interactions are possible, and similar interplanar distances have been found in pyrene and pyrene-4,5-dione.[13,14] They are tilted at an angle of about 40° to the "best plane" through the aromatic core.

In addition, the columns pile up along the *b* axis to form a layer structure like the SmC phase (Figure 4b) of the calamitic LCs. The parallel stacking causes both CO and O(*i*-C_3H_7) groups to align on the same side of the column, which does not seem to be stable due to the steric hindrance of the *i*-C_3H_7 group.[13] However, two C=O groups were found to interact with the aromatic proton on C(5) and C(5)# in the neighboring columns and vice versa. A total of four intermolecular C=O···H hydrogen bonds of 2.44 Å

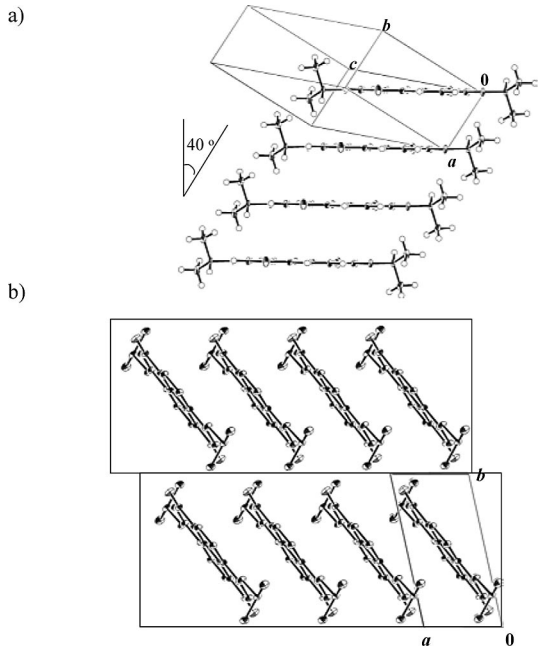

Figure 4. Crystal packings of **4e**.

per molecule should markedly stabilize the crystal structure along the molecular direction, that is, between the stacking layers (Figure 4b and Figure 5).[15]

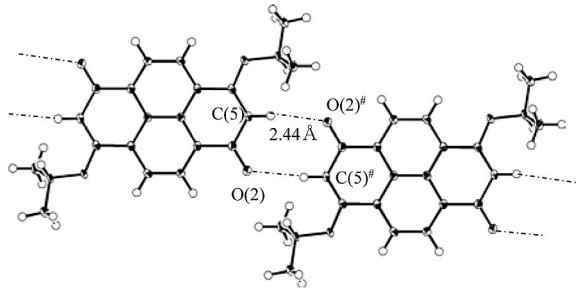

Figure 5. ORTEP drawing of **4e**.

The molecules of **5e** are stacked in parallel along the *c* axis to form a columnar structure as shown in Figure 6.[12b] The molecular distances in the column are about 3.39 and 3.42 Å, where π–π stacking interactions are also possible, and again similar interplanar distances have been determined previously.[13,14] In addition, two kinds of stacking modes were found in the column (Figure 6) and both arrangements avoid the steric hindrance of the *i*-C_3H_7 group, which is a clear difference from that of **4e**. However, the hydrogen bond between the C=O group and aromatic C(9)–H in the neighboring columns stabilizes the crystal structure (Figure 7), and this is similar to that of **4e**.

In order to accumulate information on molecular arrangement, the optical textures were studied for **4c**, **4d** and **5b**–**d** by using a polarized optical microscope (POM). As shown in Figure 8, terrace and band textures were observed for **4c** (192 °C) and **5c** (142 °C). Similar features were also observed for **4d**, **5b**, and **5d**. According to Ohta et al.[16b]

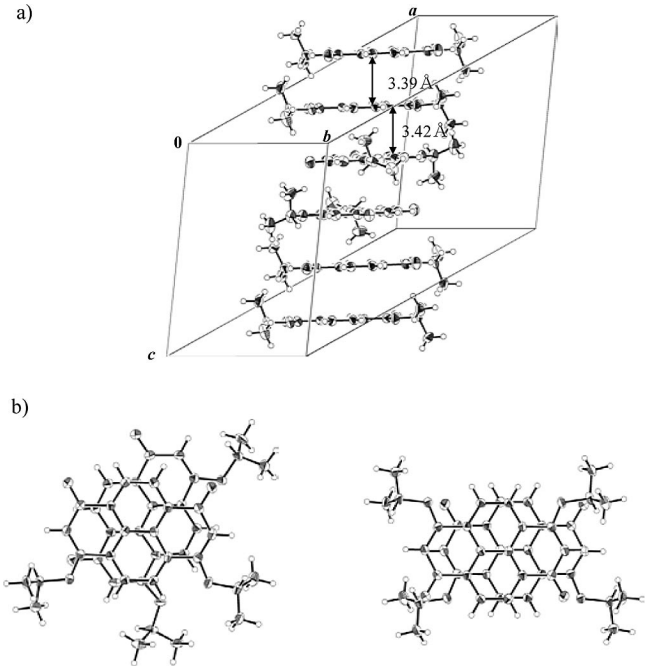

Figure 6. (a) Crystal packing and (b) π–π staking of **5e**.

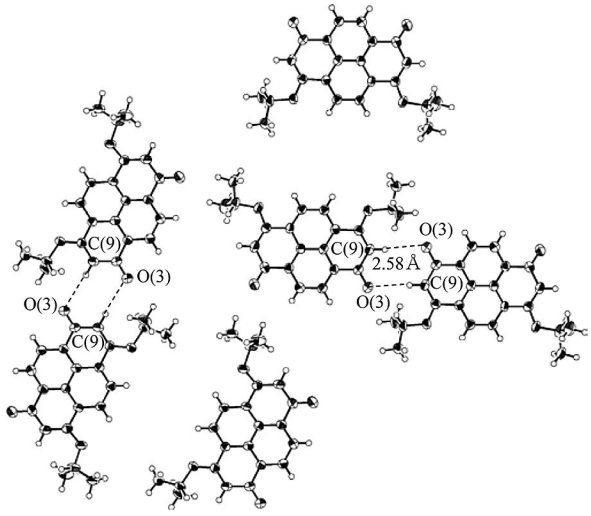

Figure 7. ORTEP drawing of **5e**.

and Billard et al.,[17] these textures can be assigned to the discotic lamellar phase D_{L2}. The D_{L2} phase is known to have both columnar and lamellar structural features, and as a result, the mesophase can show either a band texture reflecting a columnar feature or a terrace and band textures reflecting a lamellar structure.[16,17] Considering the columnar structures of **4e** and **5e** (Figures 4 and 6) and the terrace and band textures of **4c** and **5c**, their mesophases are expected to be D_{L2}. Ohta et al. discussed the fact that discotic molecules bearing four side chains tend to form lamellar phases.[16] The present study provides an example of another type of discotic molecule forming a lamellar phase with two long chains and two strongly polar groups.

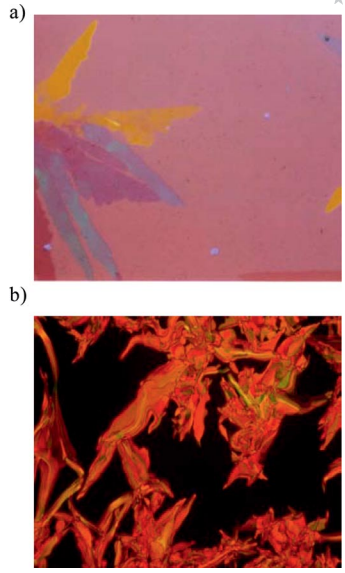

Figure 8. Polarized optical microphotograph of (a) **4c** at 192 °C and (b) **5c** at 142 °C.

The mesophase of **5c** was studied by XRD analysis at several temperatures and the results are shown in Figure 9. Figure 9a and c show an isotropic state at 150 °C and a crystalline state at 100 °C, respectively. The X-ray diagrams of **5c** at 142 °C show a set of reflections in the small-angle region and a diffuse scattering in the wide-angle region (Figure 9b). The reflections can be indexed as (00l) (l = 1, 2, 3) for 23.5, 11.8, and 7.8 Å spacings as d_{001}, d_{002}, and d_{003}, respectively, in a ratio of 1:1/2:1/3. The MOPAC calculation suggests the conformation of **5c** as that shown in Figure 3b: the fully stretched alkyl chains form an angle of

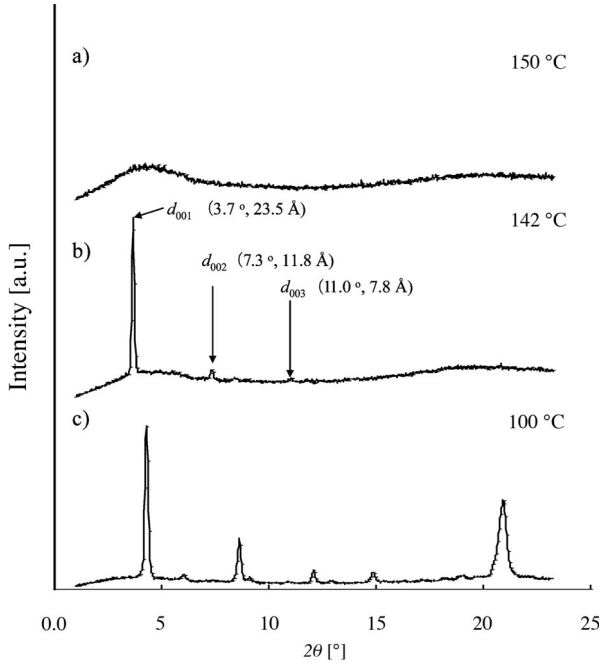

Figure 9. X ray diffractions of **5c** at (a) 150 °C, (b) 142 °C, and (c) 100 °C.

about 100°, and the distance of two long dimensions becomes ca. 23.3 Å, which well corresponds to the unit length along the *c* axis, that is, d_{001} in Figure 9b.

The X-ray diffraction pattern of **5c** suggests one-dimensional ordering, which corresponds to the lamellar structure as observed for crystalline **5e**. In contrast, the measurement of mesomorphic **4c** failed because the LC structure at 192 °C was more unstable than **5c** and only the crystalline diffractions were observed at 164 °C.

Conclusions

This article reports the synthesis of novel liquid crystalline π-acceptor pyrenediones, two *anti*-type derivatives, and three *syn*-type derivatives. In conjunction with single-crystal X-ray analyses of analogs **4e** and **5e**, the POM observations of **4c**, **4d** and **5b**–**d**, and the XRD analysis of **5c**, it is suggested that the liquid crystalline phases have terrace and band textures, characterized as D_{L2}. Detailed analysis of the LC phases and the formation of quinone–hydroquinone CT complexes are underway.

Experimental Section

General: ^{1}H NMR spectra were measured with Bruker DPX 400 and DRX 400 spectrometers (Molecular Analysis and Life Science Center (MALS), Saitama University). Chemical shifts are reported as δ values (ppm) relative to internal tetramethylsilane (TMS) in $CDCl_3$. Mass spectra were obtained with a JEOL JMS-700AM mass spectrometer (EI ionization voltage of 70 eV; MALS, Saitama University). Infrared spectra were obtained with a JASCO FTIR 125HK spectrometer.

General Procedure for the Synthesis of 4 and 5: Anhydrous iron(III) chloride (1.25 g, 7.71 mmol) was added to a mixture of **2** and **3** (500 mg, 2.15 mmol) in decyl alcohol (250 mL) at room temperature, and the temperature was raised to 120 °C. After stirring for 12 h, about 240 mL of decyl alcohol was removed under reduced pressure. The residue was diluted with water and extracted with $CHCl_3$. The organic layer was successively washed with water and brine, dried with anhydrous Na_2SO_4, and then concentrated under reduced pressure. The concentrate was chromatographed on silica gel (Kanto N60; $CHCl_3$/hexane, 3:1) to give **4c** (25%, 293 mg, 0.54 mmol) and **5c** (28%, 328 mg, 0.60 mmol). Data for **4c**: M.p. 210–212 °C. ^{1}H NMR (400 MHz, $CDCl_3$): δ = 8.48 (d, J = 7.60 Hz, 2 H, Ar*H*), 8.28 (d, J = 7.60 Hz, 2 H, Ar*H*), 6.05 (s, 2 H, Ar*H*), 4.16 (t, J = 6.40 Hz, 4 H, ArOCH_2CH$_2$CH$_2$-), 1.95 (quint, J = 6.40 Hz, 4 H, ArOCH$_2$CH_2CH$_2$-), 1.56–1.21 (m, 28 H, -CH_2-), 0.90 (t, J = 6.4 Hz, 6 H, -CH$_2$CH_3) ppm. IR (KBr): $\tilde{\nu}$ = 2950, 2920, 2850, 1640, 1610, 1560, 1340, 1230, 830 cm^{-1}. MS (EI): m/z = 544 [M]$^+$. Data for **5c**: M.p. 156–158 °C. ^{1}H NMR (400 MHz, $CDCl_3$): δ = 8.55 (s, 2 H, Ar*H*), 8.21 (s, 2 H, Ar*H*), 6.03 (s, 2 H, Ar*H*), 4.16 (t, J = 6.40 Hz, 4 H, ArOCH_2CH$_2$-), 1.95 (quint, J = 6.40 Hz, 4 H, ArOCH$_2$CH_2CH$_2$-), 1.56–1.21 (m, 28 H, -CH_2-), 0.90 (t, J = 6.40 Hz, 6 H, -CH$_2$CH_3) ppm. IR (KBr): $\tilde{\nu}$ = 3060, 2920, 1640, 1610, 1560, 1410, 1230, 830 cm^{-1}. MS (EI): m/z = 544 [M]$^+$.

4e: Prepared according to the general procedure. Yield 38%, m.p. 254–255 °C. ^{1}H NMR: δ = 8.47 (d, J = 7.60 Hz, 2 H, Ar*H*), 8.29 (d, J = 7.60 Hz, 2 H, Ar*H*), 6.04 (s, 2 H, Ar*H*), 4.77 [sext, J = 6.00 Hz, 2 H, ArOC*H*(CH$_3$)$_2$], 1.51 [d, J = 6.00 Hz, 12 H, ArOCH(CH_3)$_2$] ppm. IR (KBr): $\tilde{\nu}$ = 3020, 2950, 2860, 2850, 1640, 1610, 1560, 1340, 1230, 830 cm^{-1}. MS (EI): m/z = 348 [M]$^+$.

5e: Prepared according to the general procedure. Yield 36%, m.p. 246–248 °C. ^{1}H NMR: δ = 8.55 (s, 2 H, Ar*H*), 8.16 (s, 2 H, Ar*H*), 6.03 (s, 2 H, Ar*H*), 4.52 [sext, J = 6.00 Hz, 2 H, ArOC*H*(CH$_3$)$_2$], 1.51 [d, J = 6.00 Hz, 12 H, ArOCH(CH_3)$_2$] ppm. IR (KBr): $\tilde{\nu}$ = 2920, 2890, 1640, 1610, 1560, 1410, 1230, 830 cm^{-1}. MS (EI): m/z = 348 [M]$^+$.

Supporting Information (see footnote on the first page of this article): Characterization data of **4a**,**b**,**d** and **5a**,**b**,**d**; crystal data and structure refinement for **4e** and **5e**; ORTEP diagram of **4e** and **5e**.

Acknowledgments

M. Y. is grateful for partial financial support by theIketani Science and Technology Foundation (0181062-A).

[1] W. Brütting, *Physics of Organic Semiconductors*, John Willy & Sons, **2005**.
[2] a) D. Jerome, H. J. Schultz, *Adv. Phys.* **1982**, *31*, 299–490; b) M. R. Bryce, *Chem. Soc. Rev.* **1991**, *20*, 355–390; c) J. M. Williams, J. R. Ferraro, R. J. Thorn, K. C. Carlson, U. Geiser, H. H. Wang, A. M. Kini, M-H. Whangbo, *Organic Superconductors*, Prentice-Hall, Englewood Cliffs, New Jersey, **1992**; d) J. B. Torrance, *Acc. Chem. Res.* **1979**, *12*, 79–86.
[3] a) T. Akutagawa, G. Saitou, *Bull. Chem. Soc. Jpn.* **1995**, *68*, 1753–1773; b) K. Nakasuji, K. Sugiura, T. Kitagawa, J. Toyoda, H. Okamoto, K. Okaniwa, T. Mitani, H. Yamamoto, I. Murata, A. Kawamoto, J. Tanaka, *J. Am. Chem. Soc.* **1991**, *113*, 1862–1864.
[4] E. Leuder, *Liquid Crystal Displays: Addressing Schemes and Electro-Optical Effects*, John Willy & Sons, **2001**.
[5] a) L. L. Chapoy, D. K. Munck, K. H. Rasmussen, E. J. Dieknann, R. K. Sethi, D. Biddle, *Mol. Cryst. Liq. Cryst.* **1984**, *105*, 353–374; b) J. M. Warman, A. M. van de Craats, *Adv. Mater.* **1999**, *11*, 1469–1472; c) M. O'Neill, S. M. Kelly, *Adv. Mater.* **2003**, *15*, 1135–1146.
[6] T. Hirose, O. Kawakami, M. Yasutake, *Mol. Cryst. Liq. Cryst.* **2006**, *451*, 65–74.
[7] A. J. Fatiadi, *J. Chromatography* **1965**, *20*, 319–324.
[8] V. S. Chesnovskii, V. A. Shigalevskii, *Zh. Org. Kim.* **1986**, *22*, 1159–1163.
[9] M. Al-Ibramhim, H.-K. Roth, U. Zhokhavets, G. Gobsch, S. Sensfuss, *Solar Energy Material & Solar Cells* **2005**, *85*, 12–20.
[10] a) Y. Chen, G. Huang, C. Hsiao, S. Chen, *J. Am. Chem. Soc.* **2006**, *128*, 8549–8558; b) D. M. de Leeuw, M. M. J. Simenon, A. R. Brown, R. E. F. Einerhand, *Synth. Met.* **1997**, *87*, 53–59.
[11] a) The computations were performed with *CAChe* programs; b) M. J. S. Dewar, E. G. Zoebisch, E. F. Healy, J. J. P. Stewart, *J. Am. Chem. Soc.* **1985**, *107*, 3902–3909; c) J. J. P. Stewart, *WinMOPAC* (version 2), Fujitsu Ltd., Tokyo, Japan, **1998**.
[12] The measurements for **4e** and **5e** were performed with a Bruker SMART APEX (Saitama University, MALS Center) with Mo-K_α radiation (λ = 0.71073 Å) at 123 K. The structure was solved by direct methods and SHELXS-97 and refined by using SHELXL-97. Hydrogen atoms were located at calculated positions. Absorption correction was applied by using SADABS; a) **4e**: $C_{22}H_{20}O_4$, *Fw* 348.38, triclinic, space group $P\bar{1}$ (#2), a = 4.3861(2) Å, b = 8.9381(5) Å, c = 10.9735(7) Å, α = 79.9992(19)°, β = 87.0184(18)°, γ = 77.680(3)°, V = 413.85(4) Å^3, T = 123(2) K, Z = 1, $D_{calcd.}$ = 1.398 g cm^{-3}, μ(Mo-K_α) = 0.096 mm^{-1}, R = 0.0456 and Rw = 0.1308 for 1821 observed reflections with $I > 2\sigma$ from 1448 unique reflections; b) **5e**: $C_{22}H_{20}O_4$, *Fw* 348.38, triclinic, space group $C2/c$ (#19), a = 19.452(4) Å, b = 16.127(3) Å, c = 13.725(3) Å, β = 121.88(3)°, V = 3655.9(13) Å^3, T = 123(2) K, Z = 8, $D_{calcd.}$ =

1.266 g cm^{-3}, μ(Mo-K_α) = 0.087 mm^{-1}, R = 0.0818 and Rw = 0.2032 for 4430 observed reflections with $I > 2\sigma$ from 2876 unique reflections. CCDC-638953 and -683601 contain the supplementary crystallographic data for this paper. These data can be obtained free of charge from The Cambridge Crystallographic Data Centre via www.ccdc.cam.ac.uk/data_request/cif.

[13] G. R. Desiraju, K. V. R. Kishan, *J. Am. Chem. Soc.* **1989**, *111*, 4838–4843.

[14] Z. Wang, V. Enkelmann, F. Negri, K. Müllen, *Angew. Chem. Int. Ed.* **2004**, *43*, 1972–1975.

[15] a) G. R. Desiraju, *Acc. Chem. Res.* **1991**, *24*, 290–296; b) M. Yasutake, S. Yamaguchi, T. Hirose, *X-ray Structure Analysis Online* **2005**, *21*, x81–x82.

[16] a) K. Ohta, H. Muroki, A. Takagi, K. Hatada, H. Ema, I. Yamamoto, K. Masuzaki, *Mol. Cryst. Liq. Cryst.* **1986**, *140*, 131–152; b) K. Ohta, *Ekisho Binran* **2000**, 142–147.

[17] a) M. Giroud-Godquin, J. Billard, *Mol. Cryst. Liq. Cryst.* **1981**, *66*, 147–150; b) J. Billard, *C R. Acad. Sci. Paris* **1984**, *299*, 905–908.

Received: April 8, 2008
Published Online: July 4, 2008

